Article

Control of Quinone Redox Potentials in Photosystem II: Electron Transfer and Photoprotection

Hiroshi Ishikita, and Ernst-Walter Knapp

J. Am. Chem. Soc., **2005**, 127 (42), 14714-14720• DOI: 10.1021/ja052567r • Publication Date (Web): 30 September 2005

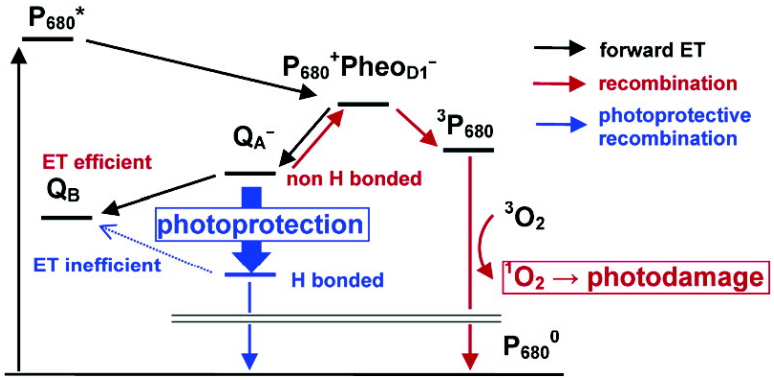

More About This Article

Additional resources and features associated with this article are available within the HTML version:

- Supporting Information
- Links to the 6 articles that cite this article, as of the time of this article download
- Access to high resolution figures
- Links to articles and content related to this article
- Copyright permission to reproduce figures and/or text from this article

View the Full Text HTML

J|A|C|S
ARTICLES
Published on Web 09/30/2005

Control of Quinone Redox Potentials in Photosystem II: Electron Transfer and Photoprotection

Hiroshi Ishikita and Ernst-Walter Knapp*

Contribution from the Institute of Chemistry and Biochemistry, Crystallography, Free University of Berlin, Takustrasse 6, D-14195 Berlin, Germany

Received April 20, 2005; E-mail: knapp@chemie.fu-berlin.de

Abstract: In O_2-evolving complex Photosystem II (PSII), an unimpeded transfer of electrons from the primary quinone (Q_A) to the secondary quinone (Q_B) is essential for the efficiency of photosynthesis. Recent PSII crystal structures revealed the protein environment of the $Q_{A/B}$ binding sites. We calculated the plastoquinone ($Q_{A/B}$) redox potentials (E_m) for one-electron reduction with a full account of the PSII protein environment. We found two different H-bond patterns involving Q_A and D2-Thr217, resulting in an upshift of $E_m(Q_A)$ by 100 mV if the H bond between Q_A and Thr is present. The formation of this H bond to Q_A may be the origin of a photoprotection mechanism, which is under debate. At the Q_B side, the formation of a H bond between D2-Ser264 and Q_B depends on the protonation state of D1-His252. Q_B adopts the high-potential form if the H bond to Ser is present. Conservation of this residue and H-bond pattern for Q_B sites among bacterial photosynthetic reaction centers (bRC) and PSII strongly indicates their essential requirement for electron transfer function.

Introduction

The photosynthetic reaction in PSII is initialized by light absorption followed by energy conversion to chemical potential at P680 chlorophyll *a* (Chl*a*), where the electronic excitation energy is used for charge separation forming a positively charged oxidized state $P680^+$. Simultaneously, an electron travels along the electron transfer (ET) chain consisting of Chl*a*, pheophytin *a* ($Pheo_{D1}$), and plastoquinones Q_A and Q_B (Figure 1). The ET from Q_A to Q_B is essential for photosynthesis. For instance, blocking this ET by herbicides, which bind in the Q_B binding pocket, stops photosynthesis, although it should be noted that the toxicity of these herbicides does not originate from the act of binding alone. The general view is that due to ET inhibition beyond Q_A the radical pairs generated by light enhance the possibility to form Chl*a* in the triplet state and leads to generation of singlet oxygen (reviewed in ref 1). Measurements of $E_m(Q_A)$ by redox titration indicated the existence of two PSII conformers with a difference of 145 mV in $E_m(Q_A)$, a low-potential Q_A form and a high-potential Q_A form.[2,3] The high-potential form yields a larger E_m difference between Q_A and $Pheo_{D1}$ (for the high-potential Q_A form, see "Q_A^- H bonded" in Scheme 1) and thus favors a direct charge recombination of $P680^+Q_A^-$ i.e., without involving the intermediate triplet generating $P680^+Pheo_{D1}^-$ state.[4] Thus, the high-potential Q_A form has been proposed to play a photoprotective role in PSII. However, the mechanism of how PSII controls $E_m(Q_A)$ is still unknown.

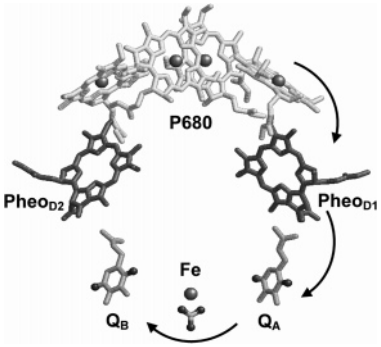

Figure 1. Forward ET in PSII.

After its double reduction and protonation, Q_B is released from its binding site to the bulk quinone pool associated with the thylakoid membrane. Double protonation of Q_B to Q_BH_2 in PSII is considered to be an event analogous to that in bRC because of the high degree of structural similarity of the reaction centers (RC) (reviewed in refs 5−7). The amino acid sequences of the corresponding proteins D1 and D2 in PSII[8] resemble subunits L and M in bRC, respectively, implying that both PSII and bRC are derived from a common ancestor.[5−7] Thus, Williams et al.[9] suggested conservation of functionality in these

(1) Rutherford, A. W.; Krieger-Liszkay, A. *Trends Biochem. Sci.* **2001**, *26*, 648−653.
(2) Krieger, A.; Weis, E. *Photosynthetica* **1992**, *27*, 89−98.
(3) Krieger, A.; Rutherford, A. W.; Johnson, G. N. *Biochim. Biophys. Acta* **1995**, *1229*, 193−201.
(4) Johnson, G. N.; Rutherford, A. W.; Krieger, A. *Biochim. Biophys. Acta* **1995**, *1229*, 202−207.
(5) Michel, H.; Deisenhofer, J. *Biochemistry* **1988**, *27*, 1−7.
(6) Baymann, F.; Brugna, M.; Mühlenhoff, U.; Nitschke, W. *Biochim. Biophys. Acta* **2001**, *1507*, 291−310.
(7) Rutherford, A. W.; Faller, P. *Philos. Trans. R. Soc. London B* **2003**, *358*, 245−253.
(8) Zurawski, G.; Bohnert, H. J.; Whitfeld, P. R.; Bottomley, W. *Proc. Natl. Acad. Sci. U.S.A.* **1982**, *79*, 7699−7703.

10.1021/ja052567r CCC: $30.25

Scheme 1. Energetics of the Forward and Backward (charge recombination) ET Processes in PSII

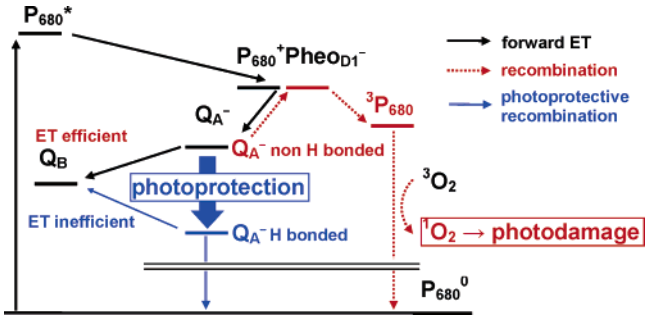

analogous parts of the two protein complexes. Therefore, structural details of PSII, especially for the D1 and D2 proteins, had been mainly provided by a series of structural modeling studies[10−14] based on the crystal structures of the L and M subunits of bRC until PSII crystal structures at higher resolutions became available. These modeling studies were useful for mutational studies of PSII. However, except for protein subunits D1 and D2, PSII and bRC differ considerably. For instance, PSII has no protein corresponding to subunit H of bRC that binds at cytoplasmic side of the L/M heterodimer (i.e., the side of RC near $Q_{A/B}$). As a consequence, the arrangement of titratable residues near Q_B in PSII differs drastically from those in bRC. A cluster of titratable residues in the neighborhood of Q_B in bRC, which is suggested to function as a proton transfer pathway to Q_B,[15] is apparently absent in PSII. Nevertheless, the corresponding proton uptake by Q_B occurs also in PSII.

To elucidate these redox reactions, we investigated the energetics of the redox reactions at $Q_{A/B}$ using the crystal structures of PSII at 3.5 and 3.0 Å resolutions (ref 16 and Loll, Kern, Saenger, Zouni, and Biesiadka, manuscript in preparation). We calculated the $E_m(Q_{A/B})$ and protonation pattern of titratable residues for each redox state of $Q_{A/B}$ in PSII based on the linearized Poisson−Boltzmann (LPB) equation, considering all atomic details of the protein environment into account. Since the calculated $E_m(Q_{A/B})$ values were affected only marginally by a change in S states of the Mn cluster (see Methods section), all of the computational results refer to the most reduced S_0 state.

Methods

Coordinates. All atomic coordinates were taken from the PSII crystal structures from the thermophilic cyanobacterium *Thermosynechococcus elongatus* at 3.5 Å resolution (3.5 Å structure).[16] We used the 3.5 Å structure to calculate $E_m(Q_A)$ and $E_m(Q_B)$ if not otherwise specified. Very recently, a newer crystal structure of PSII was obtained at 3.0 Å resolution (3.0 Å structure, Loll, Kern, Saenger, Zouni, and Biesiadka, manuscript in preparation). In this crystal structure, Q_B occupancy is relatively low. Therefore, we used the 3.0 Å structure mainly for comparison of calculated $E_m(Q_A)$. Hydrogen atom positions were energetically optimized with CHARMM.[17] During this procedure, the positions of all non-hydrogen atoms were fixed, all titratable groups were kept in their standard protonation states, that is, acidic groups ionized and basic groups (including titratable histidines) protonated, while $Chl_{D1/D2}$, Chl_Z, Pheo*a*, and $Q_{A/B}$ were kept in the neutral charge redox states. Histidines that are ligands of Chl*a* were treated as nontitratable with neutral charge.

Atomic Partial Charges. Atomic partial charges of the amino acids were adopted from the all-atom CHARMM22[18] parameter set. To account implicitly for the presence of a proton, the charges of acidic oxygens were both increased symmetrically by +0.5 unit charges. Similarly, instead of removing a proton in the deprotonated state, all hydrogen atom charges of the basic groups of arginine and lysine were diminished symmetrically by a unit charge in total. For residues whose protonation states are not available in the CHARMM22 parameter set, appropriate charges were taken from ref 19. The same cofactors' atomic partial charges were used as in previous computations of PSII.[20−22] The atomic charges of the high-spin non-heme iron (Supporting Table S1) were determined from the electronic wave functions obtained with DFT using the B3LYP functional and LACVP basis set (6-31G basis with effective core potentials on heavy atoms) as implemented in JAGUAR[23] by fitting the resulting electrostatic potential in the neighborhood of these molecules by the RESP procedure.[24]

Mn Cluster. We considered the four explicitly given μ-oxo oxygen atoms as O^{2-}, assigned each Mn ion a charge of +3.25 corresponding to the S_0 state, and included the Ca^{2+} ion and a bicarbonate that is attached to the Mn cluster, resulting in a total positive charge of +6.[20,21] All calculations refer to the S_0 state. Since the total charge of the Mn cluster depends on exact composition and charge state of its ligands, which so far are uncertain, we explored the influence of the charge state on computed $E_m(Q_{A/B})$ by increasing the total charge of the four Mn ions evenly by one unit charge to simulate an $S_n \rightarrow S_{n+1}$ transition, resulting in tiny upshifts of $E_m(Q_{A/B})$ by 7/4 mV.

Computation of Protonation Pattern and Redox Potentials. Our computation is based on the electrostatic continuum model solving the LPB equation with the program MEAD.[25] The ensemble of protonation patterns was sampled by a Monte Carlo method using Karlsberg.[26] The dielectric constant was set to $\epsilon_P = 4$ inside the protein and $\epsilon_W = 80$ for water as done in previous computations.[20−22] All computations were performed at 300 K, pH 7.0 and 100 mM ionic strength. The LPB equation was solved with a three-step grid-focusing procedure at 2.5, 1.0, and 0.3 Å resolutions. Monte Carlo sampling yielded probabilities $[A_{ox}]$ and $[A_{red}]$ of the redox states of *A*. An equal amount of both redox states ($[A_{ox}] = [A_{red}]$) was obtained with a bias potential whose value yielded the midpoint redox potential E_m. Similarly, pK_a values were computed as pH where the concentration of $[A^-]$ and $[A_{red}]$ was equal. Computed E_m are given with millivolt accuracy, without implying that the last digit is significant. To obtain the absolute value of the E_m in the protein, we calculated the electrostatic energy difference between the two redox states of $Q_{A/B}$ in a suitable reference model system where the experimental value is available. The shift of E_m in the protein relative to the reference system was then added to the experimental value for the reference system. As reference model system for plastoquinone,

(9) Williams, J. C.; Steiner, L. A.; Ogden, R. C.; Simon, M. I.; Feher, G. *Proc. Natl. Acad. Sci. U.S.A.* **1983**, *80*, 6505−6509.
(10) Trebst, A. *Z. Naturforsch.* **1987**, *42c*, 742−750.
(11) Bowyer, J.; Hilton, M.; Whitelegge, J.; Jewess, P.; Camilleri, P.; Crofts, A.; Robinson, H. *Z. Naturforsch.* **1990**, *45c*, 379−387.
(12) Svensson, B.; Etchebest, C.; Tuffery, P.; van Kan, P.; Smith, J.; Styring, S. *Biochemistry* **1996**, *35*, 14486−14502.
(13) Xiong, J.; Subramaniam, A.; Govindjee, *Protein Sci.* **1996**, *5*, 2054−2073.
(14) Xiong, J.; Subramaniam, A.; Govindjee, *Photosynth. Res.* **1998**, *56*, 229−254.
(15) Okamura, M. Y.; Paddock, M. L.; Graige, M. S.; Feher, G. *Biochim. Biophys. Acta* **2000**, *1458*, 148−163.
(16) Ferreira, K. N.; Iverson, T. M.; Maghlaoui, K.; Barber, J.; Iwata, S. *Science* **2004**, *303*, 1831−1838.
(17) Brooks, B. R.; Bruccoleri, R. E.; Olafson, B. D.; States, D. J.; Swaminathan, S.; Karplus, M. *J. Comput. Chem.* **1983**, *4*, 187−217.
(18) MacKerell, A. D., Jr. et al. *J. Phys. Chem. B* **1998**, *102*, 3586−3616.
(19) Rabenstein, B.; Ullmann, G. M.; Knapp, E. W. *Eur. Bophys. J.* **1998**, *27*, 626−637.
(20) Ishikita, H.; Knapp, E. W. *J. Am. Chem. Soc.* **2005**, *127*, 1963−1968.
(21) Ishikita, H.; Loll, B.; Biesiadka, J.; Saenger, W.; Knapp, E. W. *Biochemistry* **2005**, *44*, 4118−4124.
(22) Ishikita, H.; Knapp, E. W. *FEBS Lett.* **2005**, *579*, 3190−3194.
(23) *Jaguar4.2* ; Schrödinger, Inc.: Portland, OR, 1991−2000.
(24) Bayly, C. I.; Cieplak, P.; Cornell, W. D.; Kollman, P. A. *J. Phys. Chem.* **1993**, *97*, 10269−10280.
(25) Bashford, D.; Karplus, M. *Biochemistry* **1990**, *29*, 10219−10225.
(26) Rabenstein, B. Karlsberg online manual, 1999; http://agknapp.chemie.fu-berlin.de/karlsberg/.

Table 1. H-Bond Length for Q_A

H-bond donor to Q_A	H-Bond Length [Å] 3.5 Å structure[a]	3.0 Å structure[b]
D2-His214 ($N_{His}-O_{QA,proximal}$)	3.8	2.7
D2-Phe261 ($N_{Phe}-O_{QA,distal}$)	3.8	2.9
D2-Thr217 ($O_{Thr}-O_{QA,distal}$)	3.7	3.7

[a] From ref 16. [b] Loll, Kern, Saenger, Zouni, and Biesiadka, manuscript in preparation. Submission procedure to PDB may result in small changes of the atomic coordinates.

the value of −377 mV measured in DMF versus normal hydrogen electrode[27] was used in the E_m computation for one-electron reduction. For further information about the computation and error estimate, see previous computations for E_m[20,28] or pK_a.[29]

Results and Discussions

***$E_m(Q_A)$* in Functional PSII.** The measured $E_m(Q_A)$ values are scattered in the range from −350 to +100 mV and can be assigned to three groups of −350 to −300 mV (lowest values), −100 to 0 mV (intermediate values), and +50 to +100 mV (highest values), as reviewed in ref 3. Low $E_m(Q_A)$ values near −350 to −300 mV were found mainly in older studies,[30−32] and the assignment of the measured potentials to $E_m(Q_A)$ may be a matter of debate.[33] We obtained $E_m(Q_A) = -148$ mV in the 3.5 Å structure,[16] which can probably be assigned to the lower limit of the intermediate values of −100 mV. On the other hand, we obtained a much higher $E_m(Q_A)$ of −10 mV in the 3.0 Å structure. We did not interpret this value as belonging to the highest measured values of +50 to +100 mV, but rather attributed it to the lower limit 0 mV of the intermediate measured values. The two crystal structures are identical in the H-bond pattern for Q_A, but in the 3.0 Å structure, H bonds to Q_A are stronger than those in the 3.5 Å structure (Table 1), which upshifts the calculated $E_m(Q_A)$ for the former with respect to the latter. An interpretation of the highest measured $E_m(Q_A)$ of +50 to +100 mV is discussed later.

Varying $E_m(Q_A)$ by Flip-Flop H Bonds. The crystal structure of PSII suggests that each of the Q_A carbonyl oxygens possesses a H bond (Table 1). Optimizing hydrogen atom positions for the Q_A^0 state with CHARMM,[17] while fixing all atoms whose coordinates are given by the crystal structure[16] (see Methods section), we confirmed this H-bond pattern (Figure 2A). We also performed energy optimization of hydrogen atom positions for the Q_A^- state and found an additional weak H bond from the hydroxyl oxygen of D2-Thr217 to the proximal carbonyl oxygen of Q_A^- (O−O distance 3.7 Å (Table 1) and H−O distance 2.9 Å). D2-Thr217 is further H-bonded with the indole nitrogen of D2-Trp253 in both $Q_A^{0/-}$ charge states (Figure 2). The calculated $E_m(Q_A)$ was strongly upshifted from −148 mV in the Q_A^0 state to −52 mV upon the formation of the H bond with D2-Thr217 in the Q_A^- state. Thus, the upshift in $E_m(Q_A)$ by the H bond with D2-Thr217 amounts to 96 mV, indicating that Q_A^- is significantly stabilized by this newly formed H bond. All of these structural details described above were obtained from the 3.5 Å structure.[16] Upon the formation of the H bond with D2-Thr217, we observed an upshift of 107 mV of the computed $E_m(Q_A)$ value in the 3.0 Å structure, which is consistent with that calculated in the 3.5 Å structure. Hereby, the calculated $E_m(Q_A)$ of −10 mV in the 3.0 Å structure was upshifted to +97 mV upon H-bond formation between Q_A and D2-Thr217.

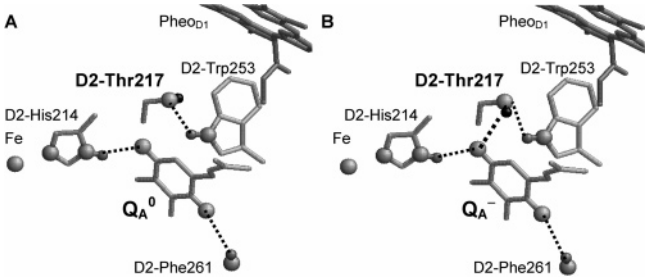

Figure 2. H-bond pattern of D2-Thr217 at Q_A in PSII. (A) No H bond in the presence of Q_A^0; (B) H bond (shown as dotted line) stabilized in the Q_A^- state. The hydroxyl hydrogen of D2-Thr217 is depicted by a dark gray sphere.

In bRC, the residues corresponding to D2-Thr217 and D2-Trp253 in PSII are fully conserved among *Rb. sphaeroides*, *Rb. capsulatus*, and *Blastochloris viridis* (*Bl. viridis*, formerly *Rhodopseudomonas viridis*). For bRC from *Rb. sphaeroides*, there are several crystal structures at relatively high resolution available, exhibiting variations in H-bond geometry at Q_A for His-M219/Thr-M222 with N−O/O−O distances of 4.8/2.4 Å,[34] 4.4/2.8 Å,[35] 3.2/3.6 Å,[36] or 2.9/3.2 Å.[37] On the basis of FTIR studies for bRC, it was proposed that a H bond at Q_A fluctuates between His-M219 and Thr-M222.[38,39] Interestingly, Breton et al. observed that in the Q_A^- state the 1650 cm^{-1} band was significantly affected upon $^1H/^2H$ exchange, while a corresponding change in the Q_A^0 state was absent. Thus, they suggested a partial shift of the H-bond partner from His-M219 for Q_A^0 to Thr-M222 for Q_A^-.[40]

We reinvestigated the situation in bRC under this aspect and found a H-bond modulation of Q_A that is analogous to the one observed in PSII. At the proximal carbonyl oxygen, Q_A^0 possesses a single H bond with His-M219. In this case, the calculated $E_m(Q_A)$ was −170 mV.[41,42] This value is close to measured $E_m(Q_A)$ at −180 mV.[43,44] However, a higher $E_m(Q_A)$ of −50 mV has also been reported.[45] Interestingly, geometry optimization of hydrogen atoms in the Q_A^- state leads to a second H bond between the proximal carbonyl oxygen of Q_A and Thr-M222. In agreement with our result, electrostatic

(27) Prince, R. C.; Dutton, P. L.; Bruce, J. M. *FEBS Lett.* **1983**, *160*, 273−276.
(28) Ishikita, H.; Knapp, E. W. *J. Biol. Chem.* **2003**, *278*, 52002−52011.
(29) Ishikita, H.; Knapp, E. W. *J. Biol. Chem.* **2005**, *280*, 12446−12450.
(30) Cramer, W. A.; Butler, W. L. *Biochim. Biophys. Acta* **1969**, *172*, 503−510.
(31) Thielen, A. P. G. M.; van Gorkom, H. J. *FEBS Lett.* **1981**, *129*, 205−209.
(32) Diner, B. A.; Delosme, R. *Biochim. Biophys. Acta* **1983**, *722*, 443−451.
(33) Rappaport, F.; Guergova-Kuras, M.; Nixon, P. J.; Diner, B. A.; Lavergne, J. *Biochemistry* **2002**, *41*, 8518−8527.
(34) Chang, C. H.; el-Kabbani, O.; Tiede, D.; Norris, J.; Schiffer, M. *Biochemistry* **1991**, *30*, 5352−5360.
(35) Yeates, T. O.; Komiya, H.; Chirino, A.; Rees, D. C.; Allen, J. P.; Feher, G. *Proc. Natl. Acad. Sci. U.S.A.* **1988**, *85*, 7993−7997.
(36) Ermler, U.; Fritzsch, G.; Buchanan, S. K.; Michel, H. *Structure* **1994**, *2*, 925−936.
(37) Stowell, M. H. B.; McPhillips, T. M.; Rees, D. C.; Solitis, S. M.; Abresch, E.; Feher, E. *Science* **1997**, *276*, 812−816.
(38) Breton, J.; Boullais, C.; Burie, J. R.; Nabedryk, E.; Mioskowski, C. *Biochemistry* **1994**, *33*, 14378−14386.
(39) Brudler, R.; de Groot, H. J. M.; van Liemt, W. B. S.; Steggerda, W. F.; Esmeijer, R.; Gast, P.; Hoff, A. J.; Lugtenburg, J.; Gerwert, K. *EMBO J.* **1994**, *13*, 5523−5530.
(40) Breton, J.; Nabedryk, E.; Allen, J. P.; Williams, J. C. *Biochemistry* **1997**, *36*, 4515−4525.
(41) Ishikita, H.; Knapp, E. W. *J. Am. Chem. Soc.* **2004**, *126*, 8059−8064.
(42) Ishikita, H.; Morra, G.; Knapp, E. W. *Biochemistry* **2003**, *42*, 3882−3892.
(43) Arata, H.; Parson, W. W. *Biochim. Biophys. Acta* **1981**, *638*, 201−209.
(44) Prince, R. C.; Dutton, P. L. *Arch. Biochem. Biophys.* **1976**, *172*, 329−334.
(45) Dutton, P. L.; Leigh, J. S.; Wraight, C. A. *FEBS Lett.* **1973**, *36*, 169−173.

computations for bRC by Zhu and Gunner[46] also implied a reorientation of the Thr-M222 hydroxyl dipole upon Q_A reduction to stabilize the negative charge. In the present study, the formation of the H bond with Thr-M222 leads to a significant upshift of $E_m(Q_A)$ by 130 mV. In the presence of this H bond, the computed $E_m(Q_A)$ is −38 mV, relatively high and close to the measured high-potential value of −50 mV in bRC.[45] Small differences in bRC sample preparation may lead to conformers with different H-bond pattern involving Q_A, thus giving rise to different $E_m(Q_A)$.

Replacing Thr-M222 by Val would turn off the H bond between Thr-M222 and Q_A without changing the size and shape of the mutated residue. This mutant would be suitable to test which of the two conformers for the Thr-M222 H bond is relevant for ET in functional bRC. Indeed, the ET from the A-branch bacteriopheophytin to Q_A proceeds for both T(M222)V mutant and wild-type bRC with the same rate constant,[47] indicating that $E_m(Q_A)$ remains unchanged upon this mutation. It is likely that the absence of the H bond between Q_A and Thr-M222/D2-Thr217 in bRC/PSII facilitates rapid ET from Q_A to Q_B because of a larger driving force. Thus, when the forward ET from Q_A to Q_B is not hampered, Q_A is unlikely to be H-bonded by Thr-M222.

Photoprotection by Shifting $E_m(Q_A)$. The Mn cluster is inactive for cells grown under dark conditions. In this case, it has been suggested that a high-potential Q_A form dominates.[2,3] Upon illumination, the inactive Mn cluster is photoactivated and PSII is transformed into a low-potential Q_A form.[4] The high-potential Q_A form can also be generated by Ca^{2+} depletion, resulting in removal of the Mn cluster.[2,3] The high-potential Q_A form (see "Q_A^- H bonded" in Scheme 1) is energetically unfavorable for ET from Q_A to Q_B as compared to the low-potential Q_A form (see "Q_A^- non H bonded" in Scheme 1) due to a smaller driving force. On the other hand, in the high-potential Q_A form the E_m difference between Q_A and $Pheo_{D1}$ is larger by 145 mV than that in the low-potential Q_A form.[2,3]

The $P680^+Pheo_{D1}^-$ state is known to generate triplet states at P680 with high yield, leading to the harmful singlet oxygen (Scheme 1). Thus, the high-potential Q_A form was proposed to play a photoprotective role since charge recombination of $P680^+Q_A^-$ occurs without involving the triplet generating $P680^+Pheo_{D1}^-$ state.[4] The existence of two competing pathways for charge recombination of the $P680^+Q_A^-$ state, originally proposed for bRC,[48,49] is supported by mutational studies varying $E_m(Pheo_{D1})$.[33] Furthermore, low values of $E_m(Q_A)$ measured in PSII were related to photodamage.[50]

Krieger et al. found that $E_m(Q_A)$ increased by 145 mV upon removal of the Mn cluster, accomplished by depletion of Ca^{2+}.[2,3] Interestingly, the measured increase in $E_m(Q_A)$ during a transition from a O_2-evolving active PSII to an inactive PSII[2,3] is similar to our computed $E_m(Q_A)$ upshift of about 100 mV upon formation of the H bond between Q_A and D2-Thr217 (see previous chapter). However, it is unclear to what extent the removal of the Mn cluster may contribute directly to the measured shift of $E_m(Q_A)$. To clarify this point, we examined the direct influence of the Mn cluster on $E_m(Q_A)$ computationally. Removing the Mn cluster by Ca^{2+} depletion eliminates the influence of these positive charges on $E_m(Q_A)$. The computed direct influence from the charges of the Mn cluster in the S_0 state upshifts $E_m(Q_A)$ by +36 mV and $E_m(Q_B)$ by +24 mV. Hence, the depletion of the Mn cluster results in downshifts of $E_m(Q_A)$ and $E_m(Q_B)$.

If we add the contributions to $E_m(Q_A)$ from the direct influence of the Mn cluster (36 mV) and from the H bond of D2-Thr217 (96 mV), the resulting total upshift of $E_m(Q_A)$ is 132 mV. This is consistent with the shift of 145 mV observed for $E_m(Q_A)$ by Krieger et al.[1−4] Thus, the additional H bond from D2-Thr217 may play a photoprotective role by providing an alternative charge recombination pathway of the $P680^+Q_A^-$ state that avoids the triplet-generating $P680^+Pheo_{D1}^-$ state (Scheme 1). Further mutational studies of D2-Thr217 will be needed to confirm this proposal.

Mechanism of the Regulation of the H-Bond Formation Itself: Dynamics of the H-Bond Flip of Thr. The main factor in $E_m(Q_A)$ regulation is a matter of debate. In the present study, we attribute the H bond with D2-Thr217 to the major factor controlling the low- or high-potential Q_A forms. If this is the case, then both the low- and high-potential Q_A forms should exist also in bRC because D2-Thr217 in PSII is conserved as Thr-M222 in bRC from *Rb. sphaeroides* (Thr-M220 for *Bl. viridis*). Consistently, recent experimental studies revealed the existence of low- and high-potential Q_A forms also in bRC from *Bl. viridis*.[51] We note that not only in bRC from *Rb. sphaeroides*[37] or in PSII,[16] which contain benzoquinones, but also in bRC from *Bl. viridis* where a naphthoquinone is in the Q_A site the hydroxyl oxygen of Thr-M220 is at a distance of 3.5 Å from the proximal carbonyl oxygen of Q_A.[52] This suggests that H-bond flip of the Thr is a common mechanism for controlling $E_m(Q_A)$ in those photosynthetic proteins.

We consider that the actual driving force of the H-bond flip of Thr is the negative charge at Q_A in the $P^+Q_A^-$ state (here, the $P^+Q_A^-$ state can also refer to the $P680^+Q_A^-$ state in PSII). Once bRC or PSII experience $P^+Q_A^-$ accumulation stabilized over a long time range, they probably become adapted to the high-potential Q_A form. From $E_m(Q_A)$ measurements of herbicide-treated PSII, Fufezan et al.[53] found that in bromoxynil-treated PSII the $E_m(Q_A)$ is lower by about 100 mV than that in DCMU-treated PSII. They also measured a shorter lifetime for the $P^+Q_A^-$ state in bromoxynil-treated PSII. Thus, they suggested that the changes in $E_m(Q_A)$ and $P^+Q_A^-$ lifetime are connected,[53] which is consistent with our proposal. Notably, the bromoxynil-treated PSII is significantly more photodamaged than the DCMU-treated PSII[53] since in this case the charge recombination pathway goes presumably via the triplet-generating $P680^+Pheo_{D1}^-$ state[4] due to the lower $E_m(Q_A)$. In the DCMU-treated PSII, presumably direct charge recombination occurs, without involving the $P680^+$ $Pheo_{D1}^-$ charge.[4]

(46) Zhu, Z.; Gunner, M. R. *Biochemistry* **2005**, *44*, 82−96.
(47) Stilz, H. U.; Finkele, U.; Holzapfel, W.; Lauterwasser, C.; Zinth, W.; Oesterhelt, D. *Eur. J. Biochem.* **1994**, *223*, 233−242.
(48) Gunner, M. R.; Robertson, D. E.; Dutton, P. L. *J. Phys. Chem.* **1986**, *90*, 3783−3795.
(49) Shopes, R. J.; Wraight, C. A. *Biochim. Biophys. Acta* **1987**, *893*, 409−425.
(50) Krieger-Liszkay, A.; Rutherford, A. W. *Biochemistry* **1998**, *37*, 17339−17344.
(51) Fufezan, C.; Drepper, F.; Juhnke, H. D.; Lancaster, C. R. D.; Un, S.; Rutherford, A. W.; Krieger-Liszkay, A. *Biochemistry* **2005**, *44*, 5931−5939.
(52) Baxter, R. H. G.; Ponomarenko, N.; Srajer, V.; Pahl, R.; Moffat, K.; Norris, J. R. *Proc. Natl. Acad. Sci. U.S.A.* **2004**, *101*, 5982−5987.
(53) Fufezan, C.; Rutherford, A. W.; Krieger-Liszkay, A. *FEBS Lett.* **2002**, *532*, 407−410.

One might argue that the accumulation of $P^+Q_A^-$ state may be promoted also by inhibition of the ET from Q_A to Q_B. In bRC, this refers to an inhibition of the conformational gating step,[54] the rate-limiting step for the first ET to Q_B. Computational studies[41,46,55] and recent ENDOR studies[56] suggested that the H-bond flip of Ser-L223 to Q_B plays an important role in the conformational gating step (discussed later). On the other hand, recent kinetic studies for the charge recombination of the $P^+Q_A^-$ state in bRC suggested that the protein−solvent relaxation stabilizing $P^+Q_A^-$ is independent of the conformational gating step.[57] This is not in conflict with the H-bond flip mechanism of Thr stabilizing the $P^+Q_A^-$ state in the present study.

Other possibilities, such as drastic reorientations of residue side chains near Q_A in response to the formation of the $P^+Q_A^-$ state, can be excluded because the recent crystal structures of Katona et al. for the $P^+Q_A^-$ and $P^0Q_A^0$ states of bRC from *Rb. sphaeroides* (PDB: 2BNS and 2BNP, respectively) revealed essentially the same orientation of residues near Q_A.[58] The predominant differences between the two bRC crystal structures in the $P^+Q_A^-$ and $P^0Q_A^0$ states are small rearrangements of the residues from Pro-H121 to Thr-H226. They suggested that these structural differences create a net electrostatic force to stabilize the Q_A^- state.[58] However, in our computation, the calculated $E_m(Q_A)$ values based on the two structures differ only by 13 mV. On the other hand, both structures were able to form the additional H bond from Thr-M222 upon Q_A^- formation with an upshift of $E_m(Q_A)$ by 43−44 mV (Ishikita, unpublished results). The only way to account for their results is that the H bond between Q_A and Thr-M222 is present in the $P^+Q_A^-$ state but absent in the $P^0Q_A^0$ state. This interpretation could be hardly obtained solely from the analysis of the crystal structures, in which hydrogen atoms are principally invisible.

Dependence of $E_m(Q_B)$ on H-Bond Pattern. According to the PSII crystal structure, both Q_B carbonyl oxygens can be involved in H bonds. The Q_B carbonyl oxygen proximal to the non-heme Fe is permanently H-bonded with N_δ of D1-His215 (N−O distance 3.4 Å). The distal Q_B carbonyl oxygen can form a second H bond with the hydroxyl hydrogen of D1-Ser264 (O−O distance 2.8 Å, O−H distance 1.9 Å) (Figure 3). However, simultaneously, the D1-Ser264 hydroxyl oxygen is able to accept another H bond from N_δ of D1-His252 (N−O distance 2.5 Å), located on the PSII stromal surface. We found a remarkable change in the H-bond pattern involving Q_B, D1-Ser264, and D1-His252, which depends not only on the redox state of $Q_B^{0/-}$ but also on the protonation state of D1-His252. In the present study, the D1-Ser264 hydroxyl hydrogen forms a H bond with Q_B^0 (O−H distance 2.0 Å) in the presence of protonated D1-His252 (Figure 3B). Simultaneously, the D1-Ser264 hydroxyl oxygen is H-bonded with N_δ of D1-His252.

In response to the redox states, Q_B^0 and Q_B^-, the geometry optimization procedure in the present study yielded subtle variations in H-bond geometry involving the side chains of D1-

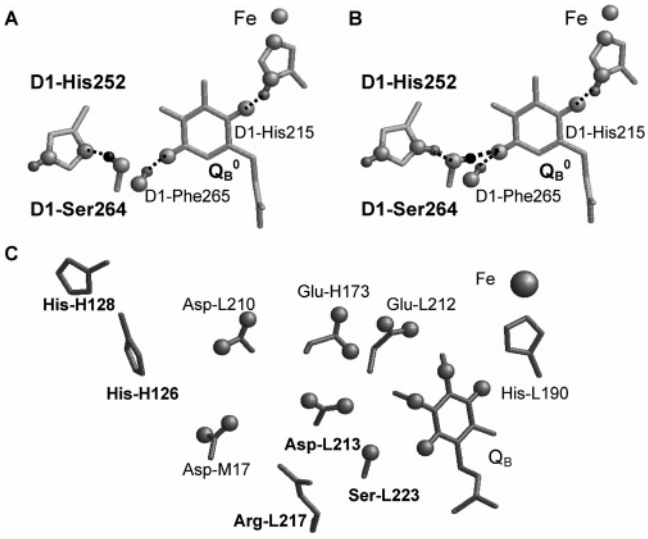

Figure 3. H-bond pattern at Q_B in PSII (A) for deprotonated D1-His252 and Q_B^0, or (B) for protonated D1-His252 and Q_B^0 or deprotonated D1-His252 and Q_B^-; (C) residues in the proton transfer pathway of bRC from *Rb. sphaeroides*.[37] The hydroxyl hydrogen of D1-Ser264 is depicted as dark gray sphere. H bonds are shown as dotted lines.

His215, D1-Ser264, and the backbone amide group of D1-Phe265. These H-bond lengths varied by about 0.1 Å with the charge state of Q_B. The calculated $E_m(Q_B)$ yielded −95 or −62 mV, depending on whether the geometry optimization of hydrogen atoms was performed in the presence of Q_B^0 or Q_B^-, respectively. Since $E_m(Q_B)$ is defined as the midpoint potential referring to an equal amount of Q_B^0 and Q_B^-, both conformations may be relevant. On the other hand, a variation of hydrogen atom positions by only 0.1 Å is within the uncertainty and accuracy level of our computational procedure. Consequently, we note that $E_m(Q_B)$ calculated in the presence of a H bond between Q_B and D1-Ser264 is in the range of −95 to −62 mV. Together with the calculated $E_m(Q_A)$ of −148 mV, these two $E_m(Q_B)$ provide an exergonic driving force of 53 and 86 meV for ET from Q_A to Q_B. From thermoluminescence studies, the free energy difference between Q_A and Q_B for one-electron reduction is estimated to be 70,[59] 80,[60] and 83 meV,[61] in agreement with our computational results.

If D1-His252 is in the charge neutral deprotonated state, the H bond of D1-Ser264 with Q_B^0 becomes weak and can be broken in the present study. Instead, the D1-Ser264 hydroxyl hydrogen is more likely to form a H bond with N_δ of D1-His252 (Figure 3A). In case of a reduced Q_B^-, however, the H bond of D1-Ser264 with Q_B exists regardless of the protonation state of D1-His252. The H bond between D1-Ser264 and Q_B^0 flip-flops with the D1-His252 protonation state, and the formation of this H bond is favored if D1-His252 is protonated. The interplay of a permanent/fluctuating H bond between $Q_B^{-/0}$ and D1-Ser264 that is coupled to the D1-His252 protonation state could explain why Q_B^- is tightly bound to its binding site[62] in contrast to the Q_B^0 in the neutral charge state. Removing the H bond between D1-Ser264 and Q_B in PSII lowered the calculated $E_m(Q_B)$ dramatically from −95 to −62 mV in the presence of this H

(54) Graige, M. S.; Feher, G.; Okamura, M. Y. *Proc. Natl. Acad. Sci. U.S.A.* **1998**, *95*, 11679−11684.
(55) Alexov, E. G.; Gunner, M. R. *Biochemistry* **1999**, *38*, 8253−8270.
(56) Paddock, M. L.; Flores, M.; Isaacson, R.; Chang, C.; Selvaduray, P.; Feher, G.; Okamura, M. Y. *Biophys. J.* **2005**, *88*, 204A.
(57) Francia, F.; Palazzo, G.; Mallardi, A.; Cordone, L.; Venturoli, G. *Biophys. J.* **2003**, *85*, 2760−2775.
(58) Katona, G.; Snijder, A.; Gourdon, P.; Andreasson, U.; Hansson, O.; Andreasson, L. E.; Neutze, R. *Nat. Struct. Mol. Biol.* **2005**, *12*, 630−631.
(59) Robinson, H. H.; Crofts, A. R. *FEBS Lett.* **1983**, *153*, 221−226.
(60) Crofts, A. R.; Wraight, C. A. *Biochim. Biophys. Acta* **1983**, *726*, 149−185.
(61) Minagawa, J.; Narusaka, Y.; Inoue, Y.; Satoh, K. *Biochemistry* **1999**, *38*, 770−775.
(62) de Wijn, R.; van Gorkom, H. J. *Biochemistry* **2001**, *40*, 11912−11922.

bond to −227 mV in its absence. A similar large downshift of $E_m(Q_B)$ was also computed for bRC from *Rb. sphaeroides*, yielding −125 mV in the presence and −231 mV in the absence of the corresponding H bond.[41] Associated with the dramatic downshift in $E_m(Q_B)$, the driving force of the ET from Q_A to Q_B vanished; that is, the ET changed from an exergonic to endergonic process with a reaction energy of about −50 and +80 meV, respectively.

Comparing PSII with bRC, the H-bond pattern at Q_B in PSII resembles the one in bRC from *Rb. sphaeroides*. In the latter, Q_B forms a H bond with the hydroxyl hydrogen of Ser-L223, depending on the protonation state of Asp-L213.[41,46,55] According to the protein sequence alignment (analysis with CLUSTAL[63]), Asp-L213 and Ser-L223 in bRC from *Rb. sphaeroides* correspond to D1-His252 and D1-Ser264 in PSII (Figure 3), pointing to a role of these residues in ET and protonation of Q_B.

Proton Uptake at D1-His252 Induced by the Formation of Q_B^-. In bRC from *Rb. sphaeroides*, a cluster of several titratable residues in the neighborhood of Q_B, namely, His-H126, His-H128, Asp-M17, Asp-L210, Glu-L212, Asp-L213, and Ser-L223, was suggested to be involved in proton transfer to Q_B, which is coupled to the ET from Q_A to Q_B (reviewed in ref 15). In D1/D2 of PSII, there are no functionally equivalent titratable residues corresponding to His-H126, His-H128, Asp-L210, and Glu-L212 in bRC, while based on protein sequence alignment (analysis with CLUSTAL[63]), Asp-L213 in bRC is replaced by D1-His252 in PSII. Nevertheless, the existence of a proton transfer chain comparable to bRC was also suggested for PSII.[65] Indeed, recent kinetic studies in PSII revealed that ET from Q_A to Q_B is significantly slower in ^2H_2O than that in ^1H_2O,[66] which strongly suggests the existence of a proton-coupled ET reaction. The PSII crystal structure[16] supports the possibility that D1-His252 with its proximity to D1-Ser264 participates in protonation of Q_B.

We found that among all titratable residues in PSII, D1-His252 changes its protonation state most significantly in response to Q_B^- formation. With formation of Q_B^-, we observed a proton uptake of 0.56 H^+ at D1-His252 in the conformer with the H bond between Q_B and D1-Ser264. On the basis of the PSII crystal structure, N_δ of D1-His252 can form a strong H bond with the hydroxyl oxygen of D1-Ser264 (N−O distance 2.5 Å); the latter forms simultaneously a H bond to the distal carbonyl oxygen of Q_B^- (O−O distance 2.8 Å) (see preceding discussion). On the other hand, the corresponding proton uptake at D1-His252 is reduced to 0.15 H^+ only when D1-Ser264 reform its H bond to D1-His252 instead to Q_B. Hence, it is likely that the formation of the H bond between Q_B and D1-Ser264 can extend the proton network from Q_B^- to D1-His252, forming a proton transfer channel from bulk solvent to Q_B^-. The corresponding Ser-L223 in bRC plays a crucial role for the ET from Q_A to Q_B and couples to proton uptake at Q_B.[41,46,55,56,67]

In the present study, the pK_a of D1-His252 is 5.9 for Q_B^0 and increases to 7.3 for Q_B^-. Interestingly, Robinson and Crofts observed a titratable residue in thylakoid membranes whose pK_a shifts by about 1.5 units upon formation of Q_B^- (pK_a 6.4/7.9 for $Q_B^{0/-}$).[68] In a similar study, the Q_B^- state was stabilized at pH 7.6,[69] implying that ET from Q_A to Q_B is coupled with proton uptake at Q_B^- involving a titratable group at this pK_a. Since no other titratable residue showed such a large pK_a change upon formation of Q_B^- in the present study, we may assume that the titratable residue found in the two experimental studies is indeed D1-His252. If this is true, ET from Q_A to Q_B should be hampered by the interruption of this proton transfer pathway. Sigfridsson et al.[70] suggested that addition of Cd^{2+} to PSII hampers ET from Q_A to Q_B, without affecting Q_A redox activity. On the basis of the PSII crystal structure,[16] they proposed that the solvent-exposed D1-His252 is involved in proton uptake at Q_B^- and a target of Cd^{2+} binding whose affinity to PSII is, however, relatively low.[70] In bRC from *Rb. sphaeroides*, the Cd^{2+} binding site is formed by Asp-H124, His-H126, and His-H128.[71] This contrasts with PSII, which possesses no other titratable residues near D1-His252 since a protein corresponding to subunit H in bRC is lacking. This might explain the low affinity of PSII to bind Cd^{2+}.

Our suggestion that D1-His252 and D1-Ser264 participate in the Q_B proton transfer network is consistent with mutant studies in which D1-Ser264 was replaced by Gly in PSII from two different species. In this mutant, it was observed that the rate of ET from Q_A to Q_B decreased in PSII from *Brassica napus*[72] and that the Q_B^- state was destabilized in PSII from *Synechocystis* PCC 6803.[73] The latter can be understood as a result of the removal of the H bond between Q_B and D1-Ser264. Therefore, we suggest that D1-His252 and D1-Ser264 are involved in proton transfer to Q_B. Proton uptake from the solvent occurs at D1-His252, while D1-Ser264 transfers the proton to the distal carbonyl oxygen of Q_B. The decrease in the rate of ET from Q_A to Q_B observed in ^2H_2O[66] may be related to proton uptake at D1-His252.

Conclusion

We investigated the influence of H bonds on $E_m(Q_{A/B})$ in PSII. The formation of a H bond from D2-Thr217 to Q_A upshifts its E_m by about 100 mV. This will be unfavorable for the forward ET from Q_A to Q_B in decreasing the driving force but will simultaneously increase the free energy gap between Q_A and $Pheo_{D1}$. The upshift of $E_m(Q_A)$ hinders backward ET via the intermediate charge state $P680^+Pheo_{D1}^-$. This promotes direct charge recombination of the radical pair $P680^+Q_A$. Thus, H-bond formation between D2-Thr217 and Q_A can play a photoprotective role in avoiding the generation of the cell poison singlet oxygen. Analogous to the flip-flop H bond between Q_B and Ser-L223 in response to the protonation state of Asp-L213 in bRC, we observed the corresponding H bond between Q_B and D1-Ser264 in response to the protonation state of D1-

(63) Higgins, D. G.; Thompson, J. D.; Gibson, T. J. *Methods Enzymol.* **1996**, *266*, 383−402.
(64) Sinning, I.; Michel, H.; Mathis, P. A.; Rutherford, A. W. *Biochemistry* **1989**, *28*, 5544−5553.
(65) Haumann, M.; Junge, W. *FEBS Lett.* **1994**, *347*, 45−50.
(66) de Wijn, R.; Schrama, T.; van Gorkom, H. J. *Biochemistry* **2001**, *40*, 5821−5834.
(67) Paddock, M. L.; Feher, G.; Okamura, M. Y. *Biochemistry* **1995**, *34*, 15742−15750.
(68) Robinson, H. H.; Crofts, A. R. In *Advances in Photosynthesis Research*; Sybesma, C., Ed.; Martinus Nijhoff/Dr. W. Junk Publishers: The Hague, 1984; Vol. 1, pp 477−480.
(69) Vermaas, W. F. J.; Renger, G.; Dohnt, G. *Biochim. Biophys. Acta* **1984**, *764*, 194−202.
(70) Sigfridsson, K. G. V.; Bernat, B.; Mamedov, F.; Styring, S. *Biochim. Biophys. Acta* **2004**, *1659*, 19−31.
(71) Axelrod, H. L.; Abresch, E. C.; Paddock, M. L.; Okamura, M. Y.; Feher, G. *Proc. Natl. Acad. Sci. U.S.A.* **2000**, *97*, 1542−1547.
(72) Bowes, J.; Crofts, A. R.; Arntzen, C. J. *Arch. Biochem. Biophys.* **1980**, *200*, 303−308.
(73) Ohad, N.; Hirschberg, J. *Plant Cell* **1992**, *4*, 273−282.

His252. The consistence of the calculated pK_a of D1-His252 for the Q_B^0/Q_B^- redox states with the experimentally observed pK_a of an nonidentified group in PSII suggests that D1-His252 could play this role in the proton uptake event at Q_B, and that the H bond from D1-His252 is able to directly regulate the E_m-(Q_B) and the driving force of the forward ET from Q_A to Q_B.

Acknowledgment. We are grateful to Drs. Biesiadka, Kern, Loll, Saenger, and Zouni for providing atomic coordinates of the PSII crystal structure at 3.0 Å resolution prior to publication. We would like to thank Drs. Biesiadka, Loll, Saenger for fruitful discussions. We also thank Drs. Donald Bashford and Martin Karplus for providing the programs MEAD and CHARMM22, respectively. This work was supported by the Deutsche Forschungsgemeinschaft SFB 498, Project A5, Forschergruppe Project KN 329/5-1/5-2, GRK 80/2, GRK 268, GRK 788/1. H.I. was supported by the DAAD.

Note added in proof. The work mentioned in the manuscript as "Loll, Kern, Saenger, Zouni and Biesiadka, in preparation" was recently published: Loll, B.; Kern, J.; Saenger, W.; Zouni, A.; Biesiadka, J. *Nature* **2005**, in press.

Supporting Information Available: Atomic partial charges for the non-heme iron complex and complete author list of ref 18. This material is available free of charge via the Internet at http://pubs.acs.org.

JA052567R